11.00 a.m., Wednesday, July 7, 1976 in Olsen Hall Invited Paper: Session: PD2

DETERMINATION OF SCATTERING LENGTHS AND MAGNETIC SPIN ROTATIONS BY NEUTRON INTERFEROMETRY

H.Rauch*, G.Badurek*, W.Bauspiess+,o, U.Bonse+, A.Zeilinger*

* Atominstitut der Österreichischen Hochschulen, Wien, Austria

+ Institut für Physik der Universität Dortmund, Germany

o Institut Laue-Langevin, Grenoble, France

RÉSUMÉ

Manipulating the optical path length of the two coherent neutron beams in a perfect crystal interferometer permits precise measurements of coherent scattering amplitudes of various elements. Experimental evaluations of the sign change of the wave function for spin 1/2-particles for a 2π-rotation and interference as well as polarization effects of nuclear and magnetic interactions are reported.

ABSTRACT

Dynamical diffraction in a suitable shaped perfect Si-crystal produces two separated monochromatic coherent beams of slow neutrons which are coherently superimposed[1,2]. Varying the thickness of the sample within the beams alters the optical path length in accordance with its index of refraction as determined by the coherent scattering length and causes a periodic intensity modulation of the emerging beam. Precise measurements of the coherent scattering length of Al, Bi, Sn, V and Nb have thus been obtained. Effects caused by the Foldy- and Schwinger-interaction and by the internal electric polarizibility of the neutron are discussed.

Using a magnetic field within one beam, the quantum mechanical hypothesis is verified that the wave function of a spin 1/2-particle changes sign by a 2π-rotation while a 4π-rotation is needed to reproduce the identical wave function. Further recent measurements of the interference and polarization effects caused by simultaneous nuclear and magnetic phase shifts will be presented. Some applications of the new technique for the determination of precipitations in alloys, the evaluation of gas content of metals, and the magnetic domain structure is mentioned.

Supported by Fonds zur Förderung der wissenschaftlichen Forschung - project 1178 and by Bundesminister für Forschung und Technologie KNF-FV-4DO 1T.

1. INTRODUCTION

At the end of 1973 we put the first powerful neutron interferometer into operation, using dynamical diffraction in a suitable shaped perfect silicon crystal[1,2]. The design principles are similar to X-ray interferometers[3,4] but here the small absorption of neutrons and the large beam size needed, result in some additional requirements concerning the crystal properties and the accurences of the dimensions.

A sketch of the Laue case (LLL) interferometer at present in use is shown in Fig.1. An incident neutron wave is coherently split and the partial waves along paths I and II are coherently superimposed at the third crystal plate. Similar to the effects of light, X-ray or electron interferometers, the wave function of one separated beam can be manipulated with regard to its amplitude and phase. The index of refraction formalism can be used for neutrons as well. As the phase of neutron waves becomes directly observable, neutron interferometry opens up new aspects in nuclear and solid state physics. The index of refraction is determining by the coherent scattering length, which is a characteristic quantity of nuclear physics. In solid state physics the influences on the interference pattern of precipitates, magnetic domains[5], gas contents etc. can be studied.

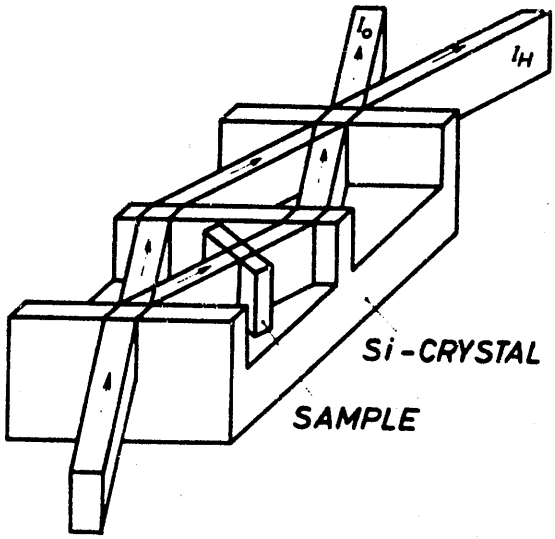

Fig.1: Sketch of the LLL-neutron interferometer

Later on, similar neutron interferometers were used by other groups for the measurement of phase shifts induced by gravity[6] and as a test of an interferometer with different thicknesses of the crystal plates[7]. The theoretical aspects of the beam formation in neutron interferometers are described in the literature[8,9,10].

Ample interest is focussed on the observation of distinct influences on the spin wave function of neutrons. Here the 4π periodicity and the appearance of the factor -1 for 2π rotations of a spinor could be demonstrated[11,12]. Recently, we observed various marked interference and polarization effects for simultaneous nuclear and magnetic phase shifts[13,14].

2. INTERFEROMETER PRINCIPLE

According to the small absorption of neutrons, both types of dynamical wave fields are present within the crystal, and form a rather complicated fringe pattern. The coherent splitting and superposition of the beams require a parallel and stable arrangement of the reflecting lattice planes and high precision of the thickness, as well as the distances between the crystal plates.

* A perfect crystal without dislocation lines, swirls and lattice constant variations is needed.
* Any rotation of the lattice planes causing deviations along the crystal in the range of the lattice constant must be balanced, and temperature inhomogeneities causing such deviations have to be avoided.

* After etching, the dimensions of the interferometer must be precise compared to the Pendelloesung length (Δ) for a considerable y range. ($\Delta = \Delta_o (1 + y^2)^{-1/2}$ with $\Delta_o = \pi \cos\theta_B / (b_c N \lambda)$, for symmetric Laue diffraction, $y = \pi(\theta_B - \theta) \sin 2\theta_B / (b_c N \lambda^2)$, θ_B ... Bragg angle, b_c ... coherent scattering length, N ... number of nuclei per unit volume, λ ... neutron wave length).
* Any vibration of the interferometer producing amplitudes in the range of the lattice constant during the flight time of the neutron through the interferometer ($t \sim 30\ \mu s$ for $\lambda = 1.8$ Å) have to be avoided. This requires a damping to a vibration level $< 10^{-4}$ g especially for low frequencies.

A sketch of the experimental arrangement as used at present at the high flux reactor in Grenoble is shown in Fig.2.

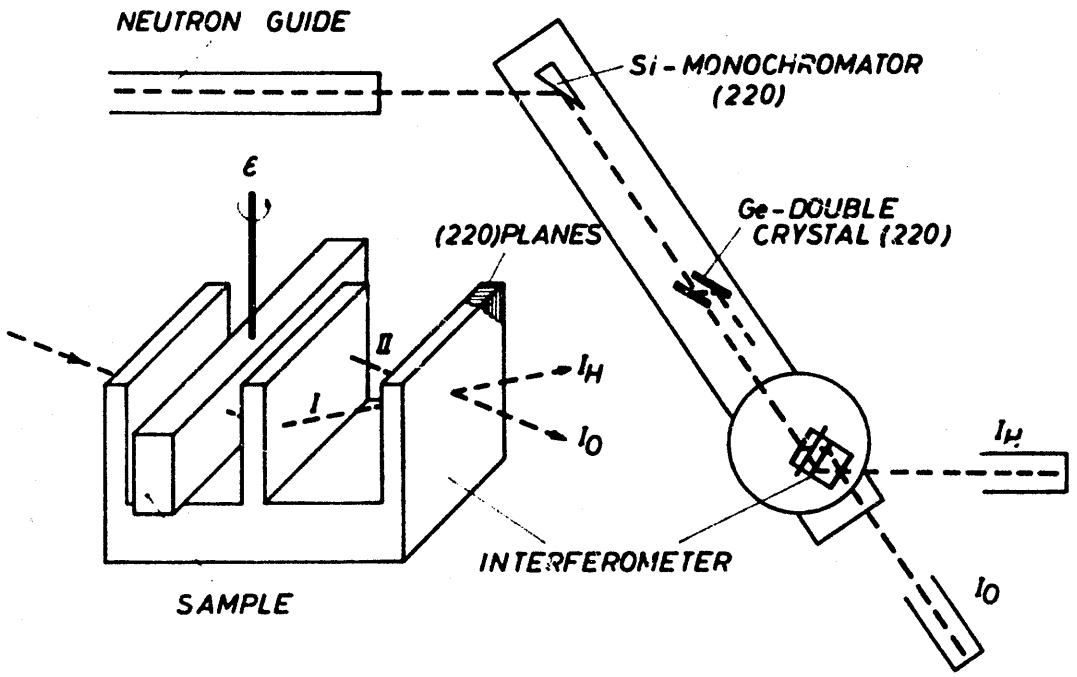

Fig.2: Sketch of the interferometer setup at the high flux reactor ILL-Grenoble.

The non dispersive double (220)-Si-reflection provides an optimal neutron utilization, and the low dispersive Si-Ge-bicrystal combination serves for precision measurements with high wave length resolution[15,16]. The interferometer has distances between the plates of about 2.73 cm and a thickness of the crystal plates of about 0.44 cm [2] and is cut from a perfect Si-crystal.

The beam behing the interferometer is formed from waves coming via paths I and II

$$I = \left| \psi^I + \psi^{II} \right|^2 \qquad (1)$$

If a phase shifting material is inserted, the interfering part of the waves behind the interferometer in the forward direction (O) obeys the relation[8,9]:

$$\frac{\psi_o^I}{\psi_o^{II}} = \exp(i\,k\,(1-n)\,\Delta D) \qquad (2)$$

The index of refraction, n, is related to the mean potential, $\bar{v}$ of the neutron within the material

$$n = 1 - \frac{\bar{v}}{2E} = 1 - \lambda^2 N b_c/(2\pi) \tag{3}$$

therefore a periodic modulation of the intensity behind the interferometer appears

$$I_o = 2\left|\psi_o^I\right|^2 (1 + \cos(2\pi\Delta D/D_\lambda) \tag{4}$$

with the λ-thickness

$$D_\lambda = 2\pi/(Nb\lambda) \tag{5}$$

By rotating a sample with the thickness D around ε (see Fig.2) the path difference ΔD is given as

$$\Delta D = D\left(\frac{1}{\cos(\theta_B+\varepsilon)} - \frac{1}{\cos(\theta_B-\varepsilon)}\right) \tag{6}$$

For a very accurate determination of b_c a lot of inaccuracies have to be taken into account. The finite wave length resolution, errors from density and thickness determination, index of refraction of air and long term drifts must be considered. With the setup in use at present, an accuracy $\Delta b_c/b_c$ of $<10^{-4}$ can be obtained and a further increase in accuracy is expected with the new and more elaborate instrument which is now under construction at ILL[16].

3. SCATTERING LENGTH

The coherent scattering length of low energy neutrons describes the mean phase shift $<\delta>$ of the wave function due to interaction $b_c = -\lim <\delta>/k$ for $k = 2\pi/\lambda$ towards zero. The neutron interaction with the whole atom contains nuclear, electromagnetic and intrinsic contributions.

$$\begin{aligned} V(r) = &- \frac{2\pi\hbar^2}{m}\left(b_{nc} + ib' + b_i \frac{\vec{\sigma}\,\vec{I}}{(I(I+1))^{1/2}}\right)\delta(\vec{r}-\vec{R}) - \\ &- \mu\vec{\sigma}\vec{H} - \frac{\hbar}{2mc}\vec{\nabla}\vec{E}\left(\mu + \frac{2mc}{\hbar}\varepsilon_2\right) - \\ &- \frac{\hbar\mu\vec{\sigma}}{mc}(\vec{E}\times\vec{k}) - \frac{1}{2}\alpha Z^2\frac{e^2}{r^4} - d\vec{\sigma}\vec{E} \end{aligned} \tag{7}$$

The first term describes the neutron nuclei interaction with a Fermi potential[17] and has a coherent (b_{nc}), an incoherent (b_i) and an absorption contribution ($b' = \sigma_a/2\lambda$). The Pauli spin matrices are represented by $\vec{\sigma}$ and $\vec{I}$ is the nuclear spin operator. The magnetic dipol interaction[18] of the magnetic moment μ with the magnetic field $\vec{H}$ of a magnetic atom or ion is given in the second expression. Then we recognize the Foldy contribution[19] due to the Zitterbewegung of the magne-

tic moment and the intrinsic charge distribution of the neutron with its second moment ε_2. The next term gives the spin-orbit-interaction[20] with the Coulomb field $\vec{E}$ of an atom. Contributions arising from an induced[21] and permanent[22] electric dipol moment of the neutron are written too. For the electric polarizability we used α; R_c denotes the cutoff radius of the Coulomb field and d is a hypothetical electric dipol moment. External gravitational, magnetic and electric fields produce further terms in Eq.(7).

By Fourier transformation taking into account the spatial charge distribution (n(r)) within an atom, the scattering length for unpolarized nuclei ($<\vec{\sigma}\vec{I}>=0$) can be written as[22,23,24]

$$b_c = b_{nc} + (\gamma r_o) f_m(\vec{Q}) <\vec{S}> (\vec{\sigma}\vec{q}) + \frac{m_e}{2m} (\gamma + \frac{\varepsilon_2}{e\mu_n}) \gamma r_o Z (1 - f(\vec{Q}))$$

$$+ \frac{m}{\hbar^2} \alpha Z^2 \frac{e^2}{R_c} + i\{ \frac{m_e}{2m} \gamma r_o Z (1 - f(\vec{Q})) (\vec{\sigma}\vec{n}) \operatorname{ctg}\frac{\theta}{2} + \qquad (8)$$

$$+ \frac{Ze(1-f(\vec{Q}))d}{\hbar \cos(\theta/2)} \frac{m}{\hbar k} \vec{\sigma}\vec{e} + \frac{\sigma_r}{2\lambda}\}$$

The symbols in Eq.(8) denote: γ ... neutron magnetic moment expressed in nuclear magnetons μ_n ($\mu = \gamma\mu_n$), r_o ... classical electron radius ($r_o = e^2/(mc^2)$), $f_m(Q)$ ... magnetic form factor and $f(\vec{Q})$ ... atomic form factor normalized to 1 for zero momentum transfer $Q = 0$, $<\vec{S}>$ ... mean magnetization, $\vec{q} = \vec{e}(\vec{e}\vec{h}) - \vec{h}$ ... magnetic interaction vector where $\vec{e}$ is a unit vector in direction of momentum transfer $\vec{e} = (\vec{k}_o - \vec{k})/2k \sin(\theta/2)$ and $\vec{h}$ is a unit vector in direction of the magnetization of the atom or ion, θ ... scattering angle, $\vec{n}$ ... unit vector perpendicular to the scattering plane $\vec{n} = (\vec{k}_o \times \vec{k})/k^2 \sin\theta$, Z ... atomic number.

The nuclear scattering length, and for magnetic materials, the magnetic dipol term are several orders of magnitude larger than the other contributions. Therefore, precision measurements for $\vec{Q} = 0$ and $\vec{Q} \neq 0$ are needed to investigate more details of the interaction. Forward scattering lengths are determined with the interferometer, therefore, a lot of terms are absent. The intrinsic contribution to the Foldy term and an experimental value for the electric polarizability are of special interest[25-28]. A phase shift of $\pi/2$ exists between the imaginary and real parts of Eq.(8). For the separation of various terms, polarized neutrons show distinct advantages.

4. EXPERIMENTAL RESULTS

The samples are rotated around ε (Fig.2) and the periodic oscillations of the O- and H-beam are measured. The standard size of the samples is about 6 x 3 x 1 cm. Fig.3 shows the results for a variety of substances where, for tin the O- and H-beam, and otherwise only the O-beam is shown. A four parameter fit with a proper error estimation gives the optimal values for the λ-thickness, oscillation amplitude etc. In most cases the contrast function $(I_H - I_O)/(I_H + I_O)$ is fitted. Figure 4 demonstrates the good quality of the fit for Sn. Table 1 shows the scattering lengths measured with the interferometer. For some substances, the accuracy of the measured values is increased compared to that discussed in the literature and in some other cases the error bars are at present determined

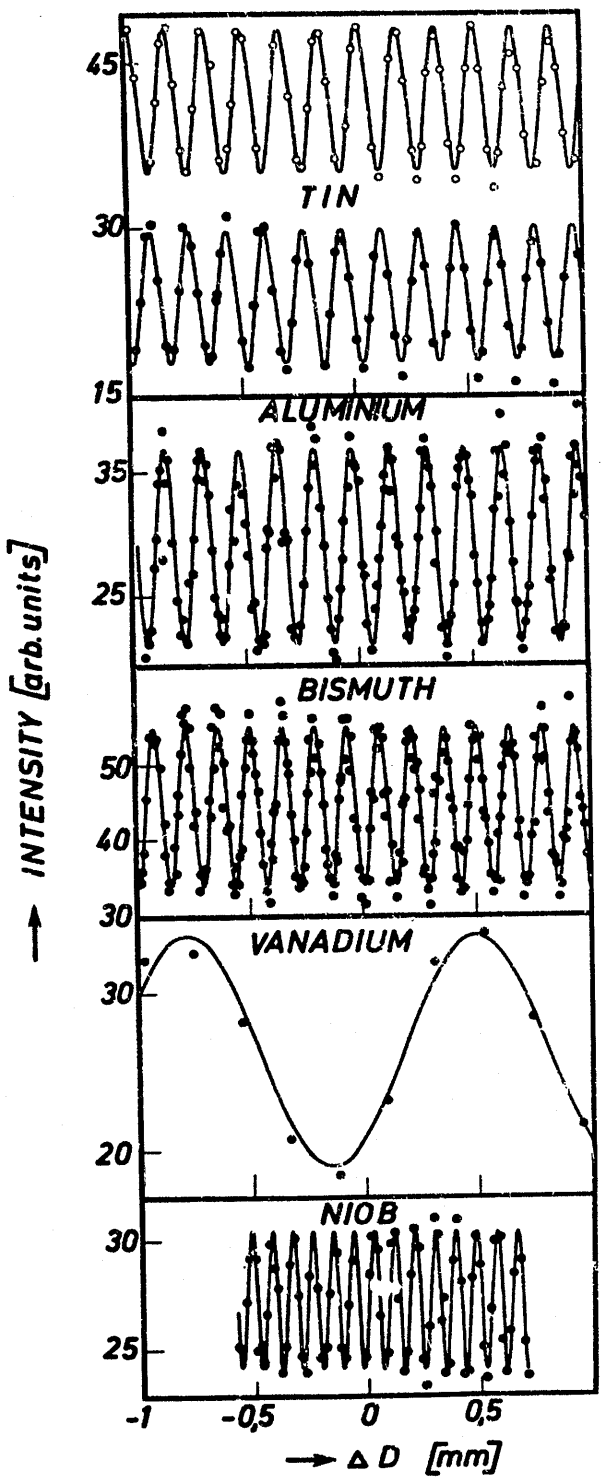

Fig.3: Characteristic intensity modulation for various metals. Open points for the H-beam and full points for the O-beam behind the interferometer.

by a preliminary, rather crude wavelength, density and impurity determination. A correction to the Debye-Waller factor is not necessary because the measurement is performed in the forward direction $Q = 0$.

To observe high order interferences, rather thick samples are inserted into

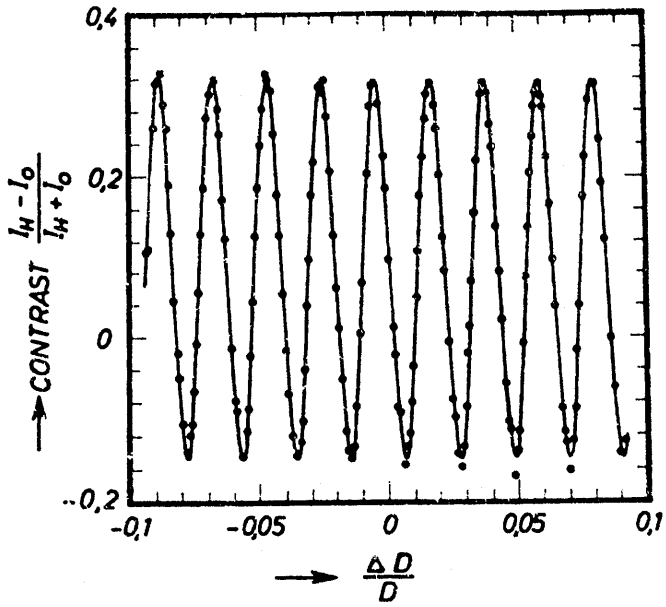

Fig.4: Fit of the measured values to the calculated curve for tin.

Table 1

	Purity (%)	N 10^{22} (cm^{-3})	λ_o (Å)	D_λ (μm)	b_c (fm)	b_c ref.[29] (fm)
Sn	99.9995	3.6990(4)	1.7860(2)	153.05(6)	6.220(2)	6.1(1)
Al	99.996	6.0204(10)	1.8322(9)	165.4(1)	3.447(5)	3.449(9)
V	99.95	7.234(10)	2.107(2)	-1012(4)	-0.408(2)	-0.48(10)
Bi	99.9995	2.821(3)	1.8264(5)	142.2(2)	8.580(8)	8.625(4)
Nb	99.99	5.542(8)	1.786(2)	89.8(1)	7.08(2)	7.11(4)

one beam. Figure 5 shows such high order (> 300) interferences, which can be interpreted as a direct measurement of the coherence length ℓ of the related wave packet ($\ell > 300\ \lambda$). An extrapolation of the contrast function gives even higher values in accordance with the wave length resolution used.

5. SPINOR ROTATION

The magnetic field couples to the magnetic moment of the neutron and causes phase shifts of the spin wave function which has for fermions a 4π periodicity[30-32] When a magnetic field B is applied to one coherent beam path the wave function is changed according to

$$\psi^{I}(\alpha) = e^{i\vec{\sigma}\vec{\alpha}/2}\ \psi^{I}(0) \qquad (9)$$

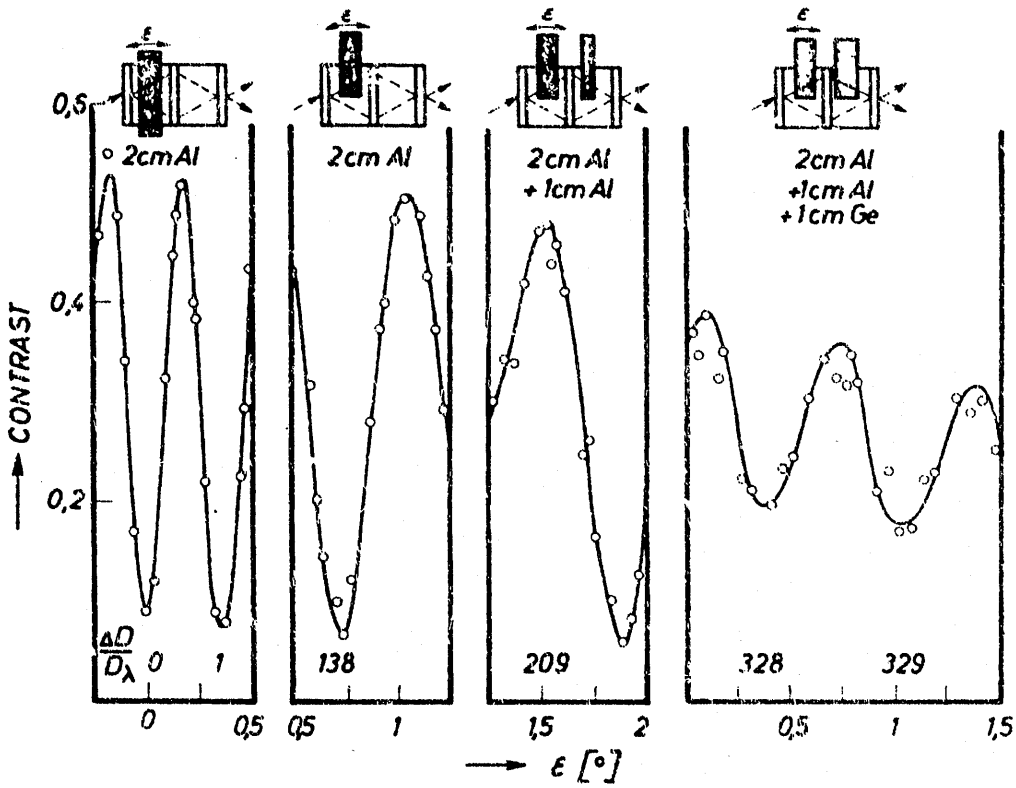

Fig.5: Observed high order interferences.

where $\vec{\alpha} = (g/v)\int \vec{B}\, ds$ is the rotation vector around the field direction. In this equation ds denotes a path element along the neutron velocity vector $\vec{v}$. Here $\vec{\sigma}$ acts on a two compound spin function. Using Eq.(9) together with Eq.(1) yields an intensity modulation.

$$\frac{I_o(\alpha)}{I_o(0)} = \frac{1 + \cos(\alpha/2)}{2} \tag{10}$$

This characteristic quantum mechanic effect which exists even for unpolarized neutrons has been observed[11,12]. The contrast function of this measurement demonstrating the typical 4π periodicity is shwon in Fig.6.

6. INTERFERENCE AND POLARIZATION EFFECTS

Characteristic interference and polarization effects arise if nuclear and magnetic phase shifts exist between the two coherent beams simultaneously[32,33]. In this case Eq.(9) reads

$$\psi^I(\alpha,\lambda) = e^{i\chi}\, e^{\pm \vec{\sigma}\vec{\alpha}/2}\, \psi^I(0,0) \tag{11}$$

The nuclear phase shift χ is given by Eq.(2) and (3) as $\chi = -N\lambda b_c \Delta D$. Again using Eq.(1) we obtain for unpolarized incident neutrons an intensity modulation

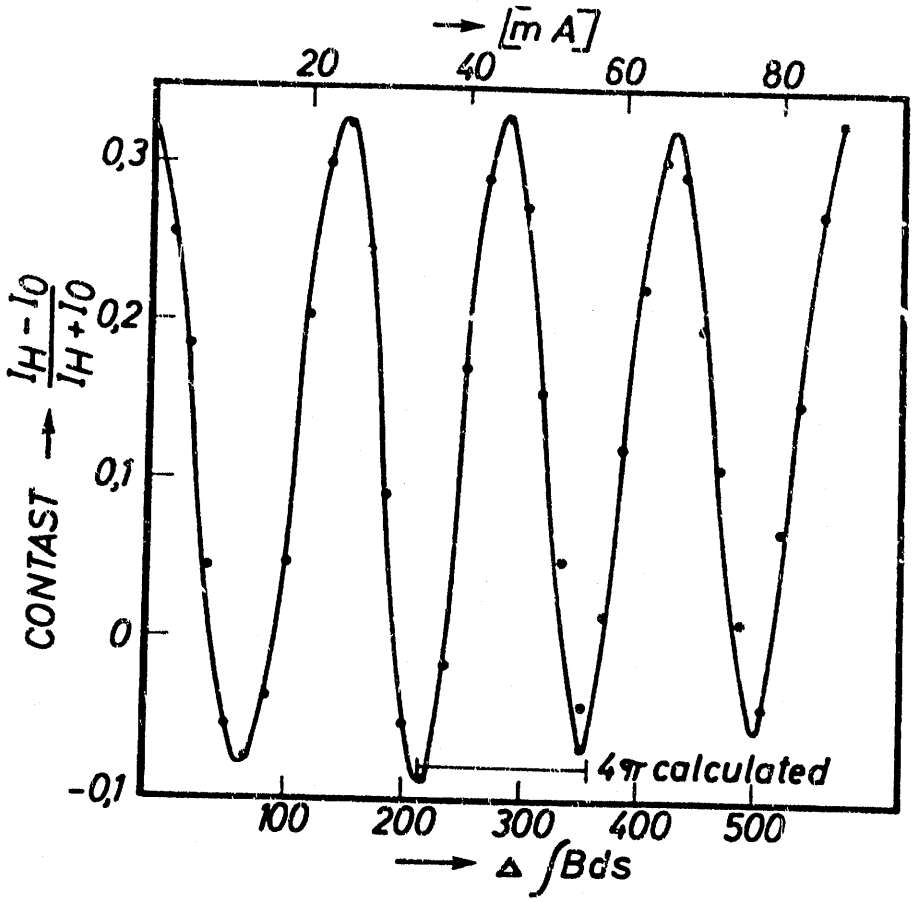

Fig.6: Observation of the 4π periodicity of a spinor. $\Delta\int B\,ds$ denotes the difference of $\int \vec{B}\,ds$ within beam path I and II.

$$\frac{I_o(\alpha,\lambda)}{I_o(0,0)} = \frac{1}{2}\,(1 + \cos\chi \cdot \cos(\alpha/2)) \tag{12}$$

and a beam polarization behind the interferometer

$$P_o = \psi_o^{I+}\,\vec{\sigma}\psi_o^{I} / \psi_c^{I+}\,\psi_o^{I} = \frac{\sin\chi\,\sin(\alpha/2)}{1 + \cos\chi\cos(\alpha/2)}\,\hat{\alpha} \tag{13}$$

where $\hat{\alpha}$ is a unit vector in the direction of $\vec{B}$.

The experimental arrangement to observe this additional intensity modulation and the beam polarization is sketched in Fig.7. Typical results for the intensity effect are shown in Fig.8 and the existing beam polarization can be seen from Fig.9[13,14]. The degree of polarization is related to the whole intensity; the interfering part of the beam is for a proper combination of the two phase shifts nearly completely polarized (99%). Many other interesting effects are expected if polarized incident neutrons and/or more sophisticated shapes of magnetic fields are used[33,34].

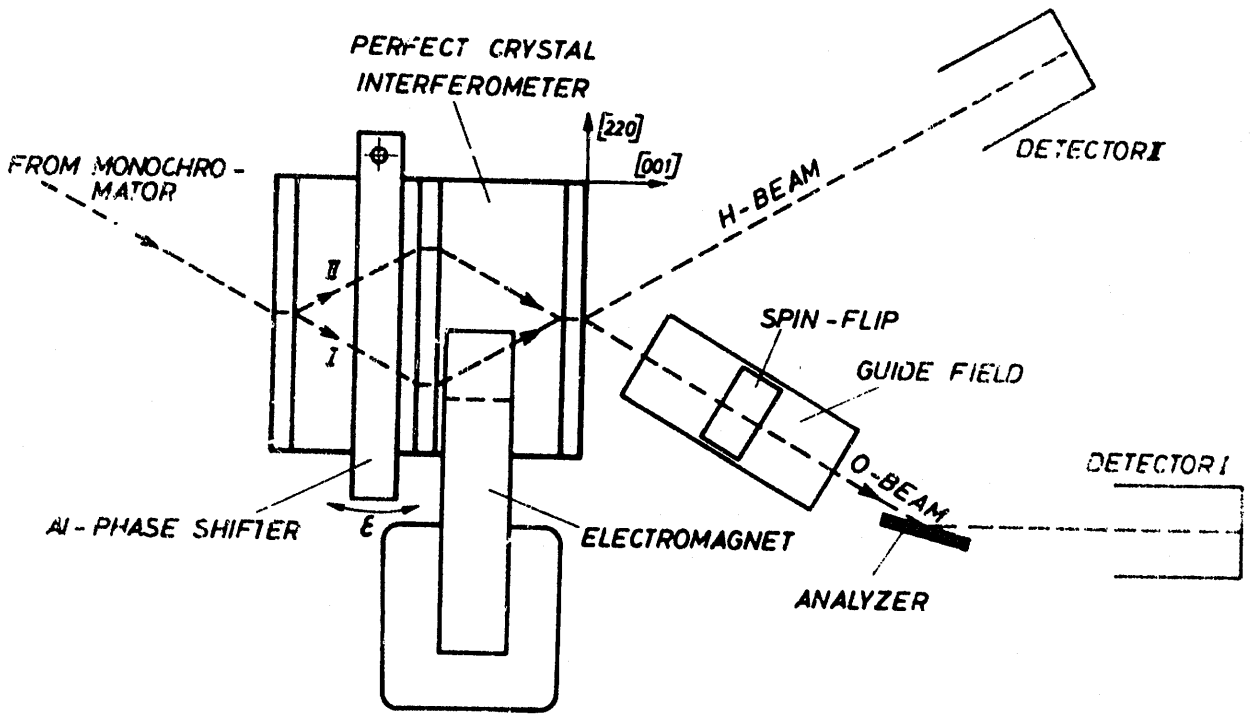

Fig.7: Arrangement for getting nuclear and magnetic phase shifts and for the observation of the beam polarization behind the interferometer.

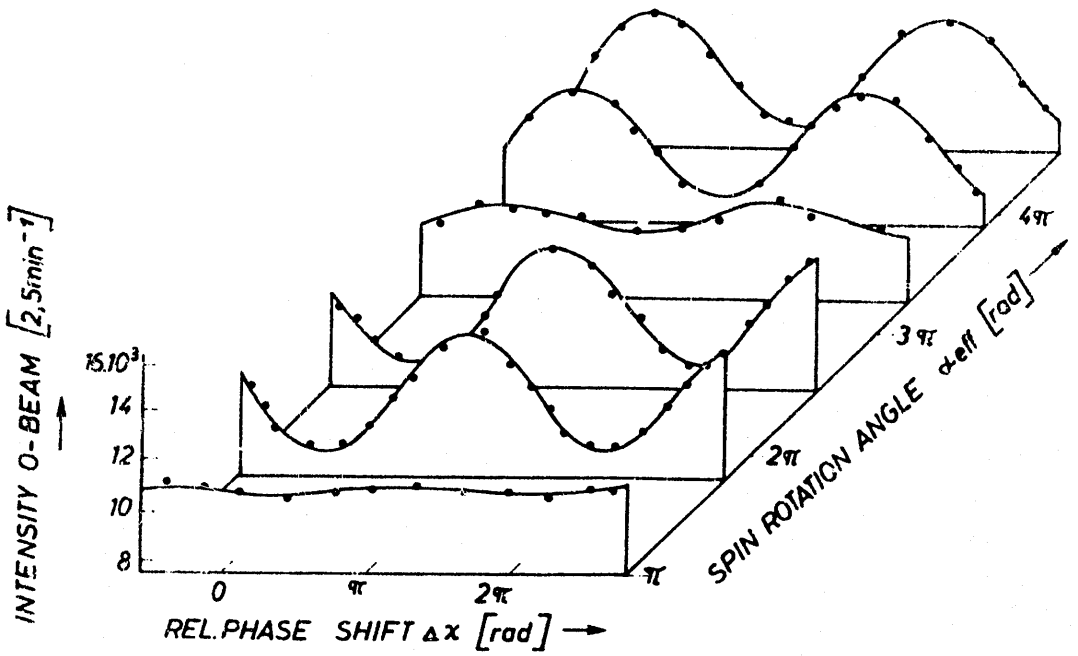

Fig.8: Measured intensity modulation for a simultaneous nuclear and magnetic phase shifts.

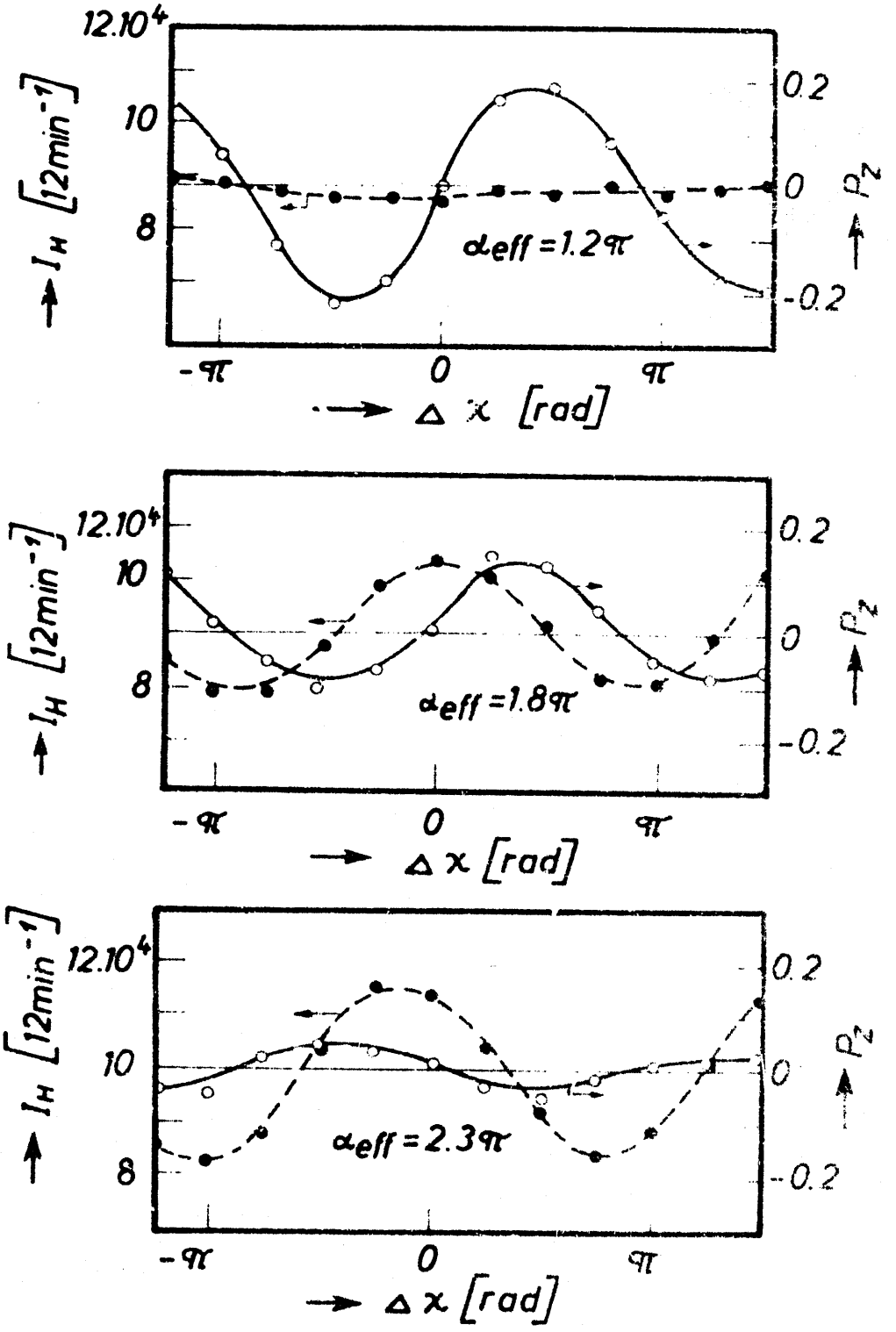

Fig.9: Correlation between the intensity and polarization modulation of the beam behind the interferometer for three different magnetic phase shifts.

7. SUMMARY

The experiments carried out so far demonstrate the capabilities of neutron interferometry. For precise measurements of scattering lengths it has become a standard method. With the interferometer forward scattering lengths are determined, therefore, a combination with other measurements ($Q \neq 0$) is necessary to isolate various contributions to the interaction.

Further nuclear physics applications appear if higher energy neutrons can be used. At least in the resonance region very significant changes of the phase shifts are expected. For such neutrons the beam separation decreases according to Bragg law and also the reflectivity decreases. The Pendelloesung length increases and defocussing effects become less serious. For 10 eV neutrons the Bragg angle is $1^{o}20'$, the reflectivity decreases to about 10% compared to 0.01 eV neutrons, and the Pendelloesung length increases by a factor of about 10. Different shapes of such perfect crystal interferometers are discussed in ref.[35] and may have distinct advantages for special problems.

The observation of the interference pattern influenced by an external gravitational or magnetic field gives information about some basic quantum mechanical phenomena. The use of polarized neutrons opens up new areas of research investigating the spin dependence of the interaction. The neutron interferometer operates always in the limit of self interferene, because the length of the wave packet is smaller, by a factor of about 10^{9}, than the mean distance between two neutrons going through the interferometer. Other applications of neutron interferometry are in the field of solid state physics and are not discussed here.

REFERENCES

1) H.Rauch, W.Treimer, U.Bonse; Phys.Lett., 1974, 47A, 369

2) W.Bauspiess, U.Bonse, H.Rauch, W.Treimer; Z.Physik, 1974, 271, 177

3) U.Bonse, M.Hart; Appl.Phys.Lett., 1965, 6, 154

4) M.Hart, U.Bonse; Phys.Today, 1970, 23, 26

5) H.Rauch, W.Schindler, W.Bauspiess, U.Bonse; 39.Physikertagung, München 1975, paper D16-2

6) R.Colella, A.W.Overhauser, S.A.Werner; Phys.Rev.Lett., 1975, 34, 1472

7) S.Kikuta, I.Ishikawa, K.Kohra, S.Hoshino; J.Phys.Soc.Japan, 1975, 39, 471

8) H.Rauch, M.Suda; phys.stat.sol.(a), 1974, 25, 495

9) W.Bauspiess, U.Bonse, W.Graeff; J.Appl.Cryst., 1976, 9, 68

10) D.Petrascheck; Acta Phys.Austr., 1976, in print

11) H.Rauch, A.Zeilinger, G.Badurek, A.Wilfing, W.Bauspiess, U.Bonse; Phys.Lett., 1975, 54A, 425

12) S.A.Werner, R.Colella, A.W.Overhauser, C.F.Eagen; Phys.Rev.Lett., 1975, 35, 1053

13) G.Badurek, H.Rauch, A.Zeilinger, W.Bauspiess, U.Bonse; Phys.Lett., 1976, 156, 244

14) G.Badurek, H.Rauch, A.Zeilinger, W.Bauspiess, U.Bonse; Phys.Rev.D, in print

15) W.Bauspiess; U. Bonse, W. Graeff, H. Fauch; Z. Phys. to be published

16) W.Bauspiess, U.Bonse, H.Rauch; Proc.Conf.Neutron Scattering, June 1976, Gatlinburg, U.S.A.

17) E.Fermi; Ricerca Sci., 1936, 1, 13

18) O.Halpern, M.H.Johnson; Phys.Rev., 1939, 55, 898

19) L.L.Foldy; Rev.Mod.Phys., 1958, 30, 471

20) J.Schwinger; Phys.Rev., 1948, 73, 407

21) R.M.Thaler; Phys.Rev., 1959, 114, 827

22) C.G.Shull, R.Nathans; Phys.Rev.Lett., 1967, 19, 384

23) C.Stassis, C.G.Shull; Phys.Rev., 1972, B5, 1040

24) W.Marshall, S.W.Lovesey; Theory of Thermal Neutron Scattering (Oxford Clarendon Press, 1971)

25) L.Koester, W.Nistler, W.Waschkowski; Phys.Rev.Lett., 1976, 36, 1021

26) L.G.Arnold; Phys.Lett., 1973, 44B, 401

27) G.V.Anikin, I.I.Kutukhov; Sov.J.Nucl.Phys., 1972, 14, 152

28) Yu.A.Aleksandrov, T.A.Machekhima, L.N.Sedlakova, L.E.Fykin; Sov.J.Nucl.Phys., 1975, 20, 623

29) Neutron Cross Sections, BNL 325, June 1973

30) H.J.Bernstein; Phys.Rev.Lett., 1967, 18, 1102

31) Y.Aharanov, L.Susskind; Phys.Rev., 1967, 158, 1237

32) A.G.Klein, G.I.Opat; Phys.Rev., 1975, D11, 523

33) G.Eder, A.Zeilinger; Nuovo Cimento, 1976, in print

34) E.Balcar; Seminar lecture, Atominstitute Vienna, 1976, private communication

35) U.Bonse; Int.Summer School X-Ray Dyn.Theory, Limoges, France, August 1975, lecture A9.

PD 2 -- DETERMINATION OF SCATTERING LENGTHS AND MAGNETIC SPIN ROTATIONS BY NEUTRON INTERFEROMETRY -- H. Rauch (Austria)

Mössbauer (Grenoble):
If you look at the forward diffracted or edge diffracted beam, you presumably use a detector which is large compared to the cross section of tha beam, or do you use one which is small? My question is really aimed at the beam profile because it won't be a perfect plaine wave. I'm sure it will have some fringe effects.

Rauch:
In the usual case it does not depend on the size of the detector because of the acceptance angle of the refraction of the third crystal plate. Therefore, all accepted particles reach the detector and in this case you really measure the forward scattering length. That is an advantage because the accuracy of scattering length determinations at present very often depend on the accuracy to which you can determine the Dybye-Waller factor. In our case the Debye-Waller factor is exactly 1, and so it is always a measurement in the forward direction. In some cases small angle scattering occurs, which contains additional information. My feeling is that this is a solid state physics application, but it has to be considered sepatately.

Robson (McGill U):
I'm most impressed by the beauty of this experiment and by the work you have done -- I'm sure everybody is. I'm also impressed by what must have been a most incredible technical feat, and in this connection I'd like to ask two questions. Firstly, is it a real problem to cut this silicon without introducing dislocations, or can anybody do it? And secondly, the thermal gradients presumably are very serious, and I was quite amazed to see that you were able to get an electromagnet in there in one of your experiments.

Rauch:
Really, the main troubles are with the production of the crystal itself, you need a perfect crystal. As far as our experiences go, we have tried to make five such crystals, and up till now only one is really working. It means that in this case you have a large enough nomogenous picture behind the crystal. Concerning the first part of your question, if you put the crystal on the goniometer you always have rotations because of the weight of the crystal itself which must be balanced. Here, X-ray pictures can help.

Regarding the temperature gradient, one has to take care that there are no gradients in temperature. Variation of temperature during long time periods doesn't matter. Therefore, the whole crystal must be very well shielded against fast temperature variation. But silicon has good conductivity for heat and so it is possible with the usual shielding to get it stable. When cutting the crystal, care must be taken to obtain accuracy in thickness and distance, and any dislocations have to be etched away afterwards. But you should not etch too much because then you lose accuracy in the distances. One knows how much is etched during a certain time and therefore it can be done rather well. At the moment, crystals available from industry have no dislocations, but there are other effects called swirls -- that is, an arrangement in some part of the crystal where the interstitial atoms have a slightly higher concentration than in the other part -- which means that you get a small variation in the lattice constants. But this is multiplied up to the last plate and then you also get an inhomogeneous picture. Even small changes of the

lattice constant produce a vertical fringe structure and you never get a homogenous picture. Similar effects occur if dislocations are present. If, for instance, you have a dislocation line, you can in no way get a homoegenous picture. That can always be demonstrated with a macroscopic system. At the moment, the main problem is to get a crystal that has the same lattice constant throughout a volume of linear dimension up to about six centimeters, which are not interesting for any electrical applications of silicon crystal as they are usually used. We hope we can get some more perfect crystals very soon.

Dabbs (O.R.N.L.):

Speaking of the purity of the crystal, you strive to obtain a very pure crystal rather than one that has been doped uniformly or in some other way.

Rauch:

If the doping is homogeneous it doesn't matter at all; because you always see the lattice plane's average. But, the problem of producing this crystal is rather difficult because you need especially for neutrons a rather large crystal. In order to get a very high contrast it is necessary to have the distances extremely accurate. At the moment we have a contrast of about 40%, but if it is possible to obtain greater precision then it seems possible to get even more contrast.

Maglich (A.N.L.)

You mentioned that you could use that same device to polarize 1-eV neutrons and I was wondering how efficient the interferometer would be? Also I would like to make a comment how impressed I was with this work and by the work of the American group which also did this rotation experiment about a year ago.

Rauch:

In response to your comment, this spin rotation experiment was performed by the American group too, I think two or three weeks later -- but almost simultaneously. In answer to your question, to get polarization it is necessary to obtain an appropriate beam division. For higher energy neutrons, the splitting will be rather small and you have to introduce a magnetized magnetic material into one beam which causes an appropriate phase shift. It is easy to calculate the right thickness. In appropriate cases you get, for instance, a completely polarized neutron beam. I would say the best way is to introduce a magnetic material where the shape is rather well defined, instead of using a magnetic field.